UCRL-JC-131218
PREPRINT

Crack Propagation in Fused Silica During UV and IR ns-laser Illumination

A. Salleo
R. Chinsio
F. Y. Génin

This paper was prepared for submittal to the
30th Annual Boulder Damage Symposium
Boulder, Colorado
September 27 - October 1, 1997

January 6, 1999

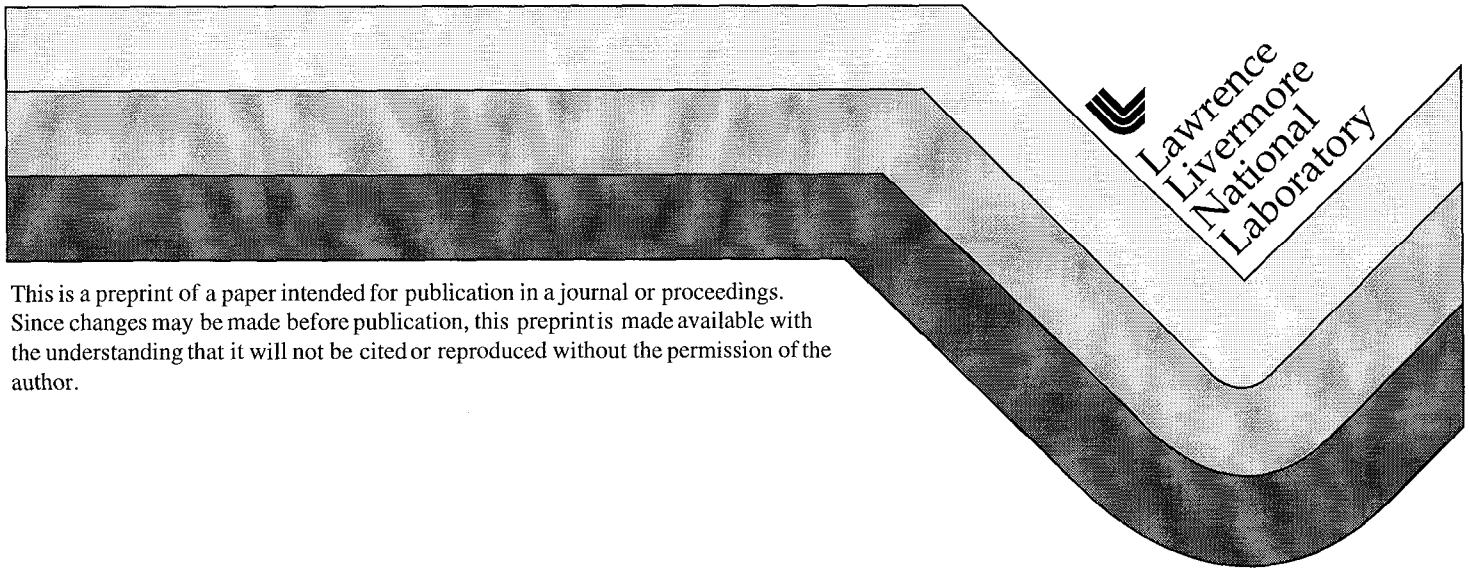

Crack propagation in fused silica during UV and IR ns-laser illumination

A. Salleo, R. Chinsio, and F. Y. Génin,

University of California, Lawrence Livermore National Laboratory,
Livermore, California 94550, U.S.A.
e-mail: fgenin@llnl.gov

ABSTRACT

The functional lifetime of large-aperture optical components used on a laser such as the National Ignition Facility is an important engineering parameter. To predict the lifetime of fused silica transmissive optics, it is necessary to measure the rate of damage propagation as a function of fluence and understand the effects of the laser parameters (e.g. wavelength and pulse width).

In order to begin such predictions without a large-area flat-top laser beam, damage growth experiments were conducted using a small (1 mm diameter) Gaussian beam. Damage was initiated by producing mechanical flaws on the surface of the optic. Since output surface damage in transmissive optics can propagate at least two orders of magnitude faster than input surface damage, the experiments were focused on damage initiated at the output surface.

The experiments showed that if damage was initiated, it could not grow at fluences below a threshold of about 5 and 8 J/cm^2 at 355 and 1064 nm, respectively. When damage was able to propagate under laser irradiation, the phenomenon occurred in two stages. Initially, the damage grew both laterally and along the optical axis at a rate varying linearly with fluence (stage I). Lateral growth stopped in areas where the fluence was lower than the growth threshold. At this point, the area of damage typically filled the size of the beam and the rate of axial damage propagation significantly decreased. During this stage (stage II), laser irradiation drilled at constant rate a channel through the window.

During stage I, the damage area grew much faster at 355 nm than at 1064 nm. During stage II, 355 nm light drilled four to five times faster than 1064 nm light. At a given fluence at 1064 nm, the drilling rate did not change between 3 ns and 10 ns. Finally, drilling at 1064 nm produced a well-defined cylindrical damaged region while 355 nm light generated less regular clusters of cracks.

1. INTRODUCTION

Optics lifetime is an important engineering parameter for the design and construction of large laser-driven inertial confinement fusion facilities. At the National Ignition Facility, transmissive optics will be mainly exposed to fundamental (λ=1064 nm) and tripled (λ=355 nm) Nd:YAG laser radiation.[1] The material of choice for transmissive optics is fused silica. The growth of laser-induced surface damage has several undesirable consequences. First, damage sites in the beam path can cause a loss in energy transmitted to the target. Second, it can scatter light and ablate or damage the structural materials in the vicinity of the optics. This in turn can contaminate the optics and initiate further damage. Finally, damage growth beyond a critical size may cause catastrophic failure of fused silica optical components (e.g. vacuum window implosion).[2] The useful lifetime of these components therefore depends largely on the rate at which damage can grow under repetitive illumination.

Lifetime predictions have been attempted on large-aperture systems (aperture area of the order of a meter square) but the lack of sufficient data to build statistical confidence hinders their interpretation. Large amounts of data can be collected using small area Gaussian laser beams (millimeter beam diameter) and small samples (e.g. 50 mm diameter). However, one must be careful when extrapolating data obtained with Gaussian small beams to predict the damage behavior of large-aperture optics irradiated by a flat-top beam.

Small beam laser-induced damage growth in silica has already been studied in the context of laser processing (particularly using pico-second laser pulses).[3-7] It was shown that under appropriate conditions, a laser beam is able to drill channels in the bulk of a silica piece. Understanding the mechanism of laser-induced damage growth is a necessary step towards the application of laser processing of transparent materials. The practical purpose of this study is to develop a physical understanding of damage growth rates rather than just provide small area data for lifetime predictions of large-aperture optics. A companion paper

in these proceedings treats the topic of lifetime predictions more directly.[8] After a brief outline of the experimental procedure, this paper describes the two stages of damage growth observed during repetitive laser illumination. The time of transition between these growth stages occurs when the damage area reaches the size of the beam. The study then attempts to characterize the effects of laser irradiation parameters (e.g. wavelength, pulse width, fluence) and of the nature of the initial defects causing damage to propagate (mechanical flaw, laser-induced damage). Finally, the damage morphologies and possible damage growth mechanisms are discussed.

2. EXPERIMENTAL PROCEDURE

Fused silica windows (diameter = 50 mm and thickness = 11 mm) were repetitively illuminated by pulsed Nd:YAG laser radiation at near-normal incidence. The shot repetition rate was 1 Hz; a preliminary study showed that growth rates were not strongly influenced by the repetition rate between 0.1 and 10 Hz. In two different sets of experiments, the fundamental (λ=1064 nm) and tripled (λ=355 nm) wavelengths were used. The laser pulses were Gaussian both temporally and spatially. The pulse-width was 8-ns at 355 nm. At 1064 nm, it was either 3-ns or 10-ns. The beam was focused in the far-field with a $1/e^2$ diameter of 1.5 mm at both wavelengths. The tests were conducted in P-polarization. The fluences reported in this study are the peak fluences of the beam.

Damage was initiated by a mechanical flaw (indentation) on the output surface. The damage dimensions (lateral area A and axial depth b) were measured as a function of the number of shots (see Fig. 1). Growth rates (i.e. change of lateral or axial damage size per shot) were deduced from these measurements. At 355 nm, for fluences below 35 J/cm^2, damage propagated from the output surface of the sample into the bulk. However, above 45 J/cm^2, damage initiated on the input surface. At 1064 nm, for the fluences studied, only output surface damage was observed.

3. RESULTS

Since the light intensity is lower at the input surface than at the output surface,[9] the laser-induced damage threshold (LIDT) of the input surface is higher than the LIDT of the output surface. When the laser fluence is higher than the LIDT of the output surface and lower than that of the input surface, damage grows from the output surface into the bulk. When the fluence is higher than the LIDT of the input surface, damage grows from the input surface into the bulk. Unless stated otherwise, the experimental data reported in this paper refer to output surface damage growth.

Figure 2 is a plot of damage depth and damage area as a function of the number of shots. Damage growth progresses in two stages. The transition between the two stages occurs when the damage area reaches the beam size. During stage I, both damage area and damage depth increase as a function of the number of shots. During stage II, only damage depth continues to grow. The laser beam then drills a cylindrical channel into the fused silica window. The damage depth grows faster during stage I than during stage II. Figure 2 shows that for 30 J/cm^2, 1064 nm, 10-ns pulse can grow damage depth about four times faster during stage I than stage II. Finally, the nature of damage propagation calls for stage II to be referred to as a drilling stage.

3.1 Stage I damage propagation

The damage area as a function of the number of shots at 1064 and 355 nm is plotted in Figs. 3 and 4, respectively. Figures 5 and 6 show the damage depth as a function of the number of shots for the same set of experiments. In these plots, the transition between the two damage growth stages is quite clear.

First, damage does not propagate from a mechanical flaw (indentation or scratch) below a threshold of about 5 and 11 J/cm^2 at 355 and 1064 nm. If damage is initiated by a high fluence shot, the damage growth threshold at 1064 nm drops to about 8 J/cm^2. These numbers are consistent with earlier studies which showed that below 5 J/cm^2, damage initiated by output surface contamination particles at 355 nm is stable.[10]

At a given laser wavelength, the damage depth increases linearly with the number of shots. The end of stage I is marked by a significant reduction in depth growth rate. At constant fluence, the damage grows

more quickly at 355 than at 1064 nm. Furthermore, the diameter of the damaged zone exceeds the $1/e^2$ beam diameter at the end of stage I at both wavelengths. Since the damaged area is nearly circular, a damage diameter d can be extracted from the previous data. Figures 7 and 8 show the damage aspect ratio (diameter divided by depth) as a function of the number of shots during stage I. The damage aspect ratio is fairly constant; 1.3 at 1064 nm, and 2.0 at 355 nm. Such aspect ratio is likely to be strongly influenced by the shape of the beam. For a Gaussian beam, it is anticipated that the ratio be smaller than for a flat-top beam since the fluence decreases with distance from the axis of the beam.

3.2 Stage II drilling

Stage II begins once damage only grows along the direction of the optical axis and lateral growth stops. At constant fluence, the beam drills into the bulk of fused silica at constant rate. Figure 9 shows the growth rate as a function of fluence at 1064 and 355 nm. No drilling at a mechanical flaw occurs below 5 J/cm^2 at 355 nm and 11 J/cm^2 at 1064 nm. Above these drilling thresholds, the drilling rate increases linearly with fluence at both wavelengths. At a given fluence, drilling occurs always faster at 355 than at 1064 nm. Figure 10 shows that at an increase in pulse-width from 3-ns to 10-ns 1064 nm does not seem to influence the drilling rate (within the fluence range investigated here).

Figure 11 illustrates how the drilling rate at a fixed site of the sample (1064 nm; 10 ns) can vary as a function of fluence and how the nature of the damage initiation defect can influence the drilling threshold. Laser damage was first initiated at a mechanical flaw. The fluence was gradually increased above the onset of drilling (point A) where the drilling rate jumped to about 4 μm/shot (point B). The drilling rate then increased linearly (to point C) and decreased (along C-D) until drilling stopped (point D). The drilling rate as a function of fluence shows an hysteresis. This hysteresis disappears when the same experiment is carried out on a laser-damaged site as a precursor of damage growth rather than a mechanical flaw.

During stage II, the damage morphology consists of narrow channels. Figure 12 shows that at 1064 nm, a 30 J/cm^2 peak fluence beam drills wider channels than a 20 J/cm^2 peak fluence beam. At a given fluence and beam size, 355 nm radiation causes more cracking than 1064 nm radiation (Fig. 13).

Laser drilling from the front side shows a different morphology. Front side drilling does not produce visible cracks but rather a smooth-walled molten channel (Fig. 14). Front side drilling was found to occur at a rate two orders of magnitude slower than backside drilling.

4. DISCUSSION

Stage I is characterized by axial and lateral damage growth. The damage aspect ratio (i.e. diameter to depth ratio) remains roughly constant as damage dimensions increase (Figs. 7 and 8). At 355 nm, damage is nearly hemispherical (average aspect ratio of about 2) while at 1064 nm damage is more elongated in the axial direction (ratio of about 1.3). Damage area saturation marks the onset of stage II (Fig. 2). The aspect ratio is likely to be strongly influenced by the shape of the beam (Gaussian vs. flat-top). While the damage is shallow, the potential for stress relief at the surface may also influence the path of damage propagation. During the final stage of drilling, as the drilled channel is about to break through the input surface, damage growth was found to accelerate. Figure 15 illustrates schematically how the drilling rate varies as drilling progresses through the thickness of the silica window. Figures 3 through 6 indicate that output surface damage growth is more severe at shorter wavelengths and at higher fluences.

At 1064 nm, stage II drilling rate does not depend on pulse width; this observation should be verified with longer pulse-width and at other wavelengths. Unlike the damage threshold,[10] the drilling rate only depends on the total energy input and not on the energy deposition rate (Fig. 10). This indicates that laser drilling may occur well after the laser pulse is over.

The hysteresis shown in Fig. 11 can be explained in terms of damage precursors. At point A, drilling is initiated at a mechanical flaw at about 11 J/cm^2. When the fluence is increased, the drilling rate jumps from 0 to about 4 μm/shot and follows the linear segment B-C in Fig. 11. If the fluence is decreased, the drilling rate decreases along the segment C-D. Finally, if the fluence is increased again, drilling can resume along the same segment at only 7 or 8 J/cm^2. This clearly points out the difference in drilling threshold between a mechanical flaw and a laser-induced flaw. This may also indicate that the laser light does not simply crack fused silica. Fused silica may have undergone a transformation upon laser irradiation. Figure

16 shows several scanning electron micrographs of the debris found inside a channel drilled at 1064 nm. The debris seems to have melted (round particles). As damage growth requires absorption of energy, two mechanisms for such absorption can be thought of. On one hand, light can be locally enhanced by cracks in fused silica.[12] Since cracks are also mechanical weak spots, this could explain why the damage threshold of a mechanical flaw (about 11 J/cm^2 at 1064 nm, 10-ns) is much lower than the damage threshold of a polished fused silica surface (about 60 J/cm^2 at 1064 nm, 10-ns). On the other hand, laser damaged fused silica may be slightly more absorbing thus transferring laser energy into the sample more effectively and damaging it at lower fluences.

For a Gaussian beam, as peak fluence increases, the $1/e^2$ diameter remains constant (by definition). However, the diameter of the region above a cut-off fluence increases with increasing peak fluence. Figure 12 shows that at 1064 nm, the diameter of the drilled channel increases with fluence and that its rim coincides with the location where the fluence is about 8 J/cm^2 (regardless of the beam peak fluence). Since the drilling threshold at laser-damaged sites falls between 7 and 8 J/cm^2 (see Fig. 11), the diameter of the channel seems to be mainly determined by this threshold. For a Gaussian beam, the continuously varying intensity profile therefore imposes a cut-off in the damage width. On the other hand, for a flat-top beam, lateral damage growth is predicted to increase continuously during irradiation above the drilling threshold.

At 355 nm, the drilling morphology consists of clusters of cracks centered along the beam optical axis (see Fig. 13). The cracks tend to occur in a more irregular fashion and it becomes more difficult to define or determine precisely the channel width. This observation and the higher drilling rate indicate that for a given fluence, more energy is deposited into the sample at 355 nm than at 1064 nm.

Finally, for the collimated beam used in the study, front side drilling occurred more easily at 355 nm than 1064 nm. The onset of front side drilling typically inhibits backside drilling. The plasma ignited at the front side shields the material downstream from the beam. The front side drilling cone shown in Fig. 14 has the typical shape of ablation craters.[13-15]

5. CONCLUSIONS

The growth of laser-induced damage at 355 nm and 1064 nm in fused silica under small (1 mm diameter) Gaussian beam irradiation occurs in two stages. First, damage grows both laterally and along the optical axis, as long as the size of lateral damage is less than the beam size (stage I). The growth rate is linear with fluence. Damage stops to grow at fluences below a threshold of 5 and 8 J/cm^2 at 355 and 1064 nm, respectively. Above these threshold fluences, once the damaged zone fills the irradiated area, damage only grows along the optical axis (laser drilling mode, stage II). At 1064 nm, the rim of the damaged cylinder corresponds to the location where the fluence is higher than the drilling threshold of 8 J/cm^2. The diameter of the drilled channel at 1064 nm therefore depends on the intensity profile of the beam and on the damage growth threshold of the material. The damage aspect ratio is constant during stage I (1.3 at 1064 nm and 2.0 at 355 nm). For flat-top beams, this ratio should be higher since the fluence does not drop with distance from the center (lateral growth is expected to propagate faster).

The early phase of stage I data could be used to predict damage growth in large-aperture optics, where the damage size is always smaller than the beam size, but such data has to be scaled to take the beam shape into account. On-going work with a larger flat-top beam (5 mm x 5 mm) will allow us to extend stage I growth results at both 355 and 1064 nm and obtain data to predict large-aperture optics lifetime.

During stage I, the damage area grows much faster at 355 nm than at 1064 nm. During stage II, 355 nm light drills four to five times faster than 1064 nm light. At a given fluence at 1064 nm, the drilling rate does not change between 3 ns and 10 ns. This lack of dependence on pulse-width should be confirmed by experiments at shorter or longer pulse widths. Finally, drilling at 1064 nm produces a well-defined cylindrical damaged region while 355 nm light generates less regular clusters of cracks.

6. ACKNOWLEDGMENTS

This work was performed under the auspices of the U.S. Department of Energy by Lawrence Livermore National Laboratory under contract No. W-7405-Eng-48. The authors want to acknowledge very useful discussions with Drs. J. H. Campbell, M. D. Feit, A. M. Rubenchik, M. R. Kozlowski, and Z. Wu.

7. REFERENCES

1. National Ignition Facility Conceptual Design Report, Lawrence Livermore National Laboratory, *Report No. UCRL-PROP-117093* (1994).

2. J. H. Campbell, P. A. Hurst, D. D. Heggins, W. A. Steele, and S. E. Bumpas, "Laser induced damage and fracture in fused silica vacuum windows", in Laser-Induced Damage in Optical Materials, *SPIE* **2966**, 106-125 (1997).

3. H. Varel, D. Ashkenasi, A. Rosenfeld, M. Wähmer, and E. E. B. Campbell, "Micromachining of quartz with ultrashort laser pulses", *Appl. Phys. A* **65**, 367-373 (1997).

4. H. Varel, D. Ashkenasi, A. Rosenfeld, R. Herrmann, and E. E. B. Campbell, "Laser-induced damage in SiO_2 and CaF_2 with picosecond and femtosecond laser pulses", *Appl. Phys. A* **62**, 293-294 (1996).

5. D. Ashkenasi, A. Rosenfeld, H. Varel, M. Wähmer, and E. E. B. Campbell, "Laser processing of sapphire with picosecond and sub-pico-second pulses", *Appl. Surf. Sci.* **120**, 65-80 (1997).

6. S. Ameer-Beg, W. Perrie, S. Rathbone, J. Wright, W. Weaver, and H. Champoux, "Femtosecond laser microstructuring of materials", *Appl. Surf. Sci.* **127-129**, 875-880 (1998).

7. H. Hornberger, R. Weissmann, and N. Lutz, "Machining of silica glasses using eximer laser radiation", *Glass Sci. and Technol.* **69**, 44-49 (1996).

8. M. D. Feit, A. M. Rubenchik, M. R. Kozlowski, F. Y. Génin, S. Schwartz, and L. Sheehan, "Extrapolation of damage test data to predict performance of large-area NIF optics at 355 nm", in these proceedings.

9. M. D. Crisp, N. L. Boiling and G. Dubé, "Importance of Fresnel reflections in laser surface damage of transparent dielectrics", *Appl. Phys. Lett.* **21**(8), 364-366 (1972).

10. F. Y. Génin, M. R. Kozlowski, and R. M. Brusasco, "Catastrophic failure of contaminated fused silica optics at 355 nm", in Second Annual International Conference on Solid State Lasers for Application to Inertial Confinement Fusion, *SPIE* Vol. **3047**, 978 (1997).

11. B. C. Stuart, S. Herman, M. D. Perry, "Laser-induced damage in dielectrics with nanosecond to subpicosecond pulses. I. Experimental", in Laser-Induced Damage in Optical Materials, *SPIE* **2428**, 568-578 (1994).

12. N. Bloembergen, "Role of Cracks, Pores, and Absorbing Inclusions on Laser-Induced Damage Threshold at Surfaces of Transparent Dielectrics", *Appl. Optics* **12**(4), 661-664 (1973).

13. A. M. Rubenchik, L. B. Da Silva, M. D. Feit, S. Lane, R. A. London, M. D. Perry, and B. C. Stuart, "Dental tissue processing with ultra-short pulse laser ", in Biomedical Optics 96, *SPIE* **2672**, 222-229 (1996).

14. B. C. Stuart, M. D. Feit, S. Herman, A. M. Rubenchik, et al., "Optical ablation by high-power short-pulse lasers", *J. Opt. Soc. of Am. B* **13**, 459-68 (1996).

15. B. C. Stuart, M. D. Perry, M. D. Feit, L. B. Da Silva, and A. M. Rubenchik, "New Machining of biological materials, dielectrics and metals with femtosecond lasers", Trends in Optics and Photonics, Lasers and Optics for Manufacturing **9**, 94-98 (1996).

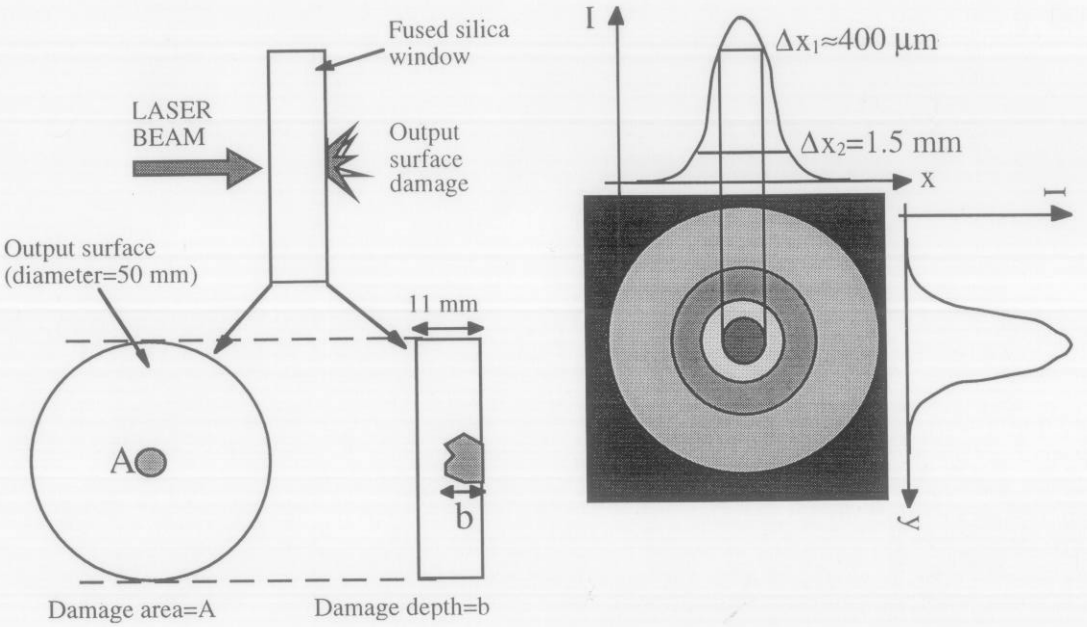

Figure 1: Sketch defining the quantities measured during this study. The Gaussian beam profile is shown on the right; the $1/e^2$ diameter of the beam is about 1.5 mm.

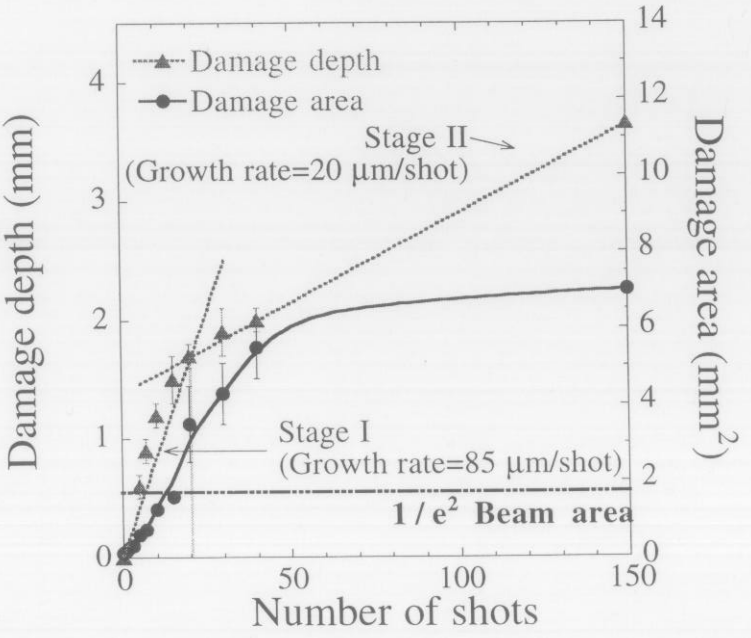

Figure 2: Damage depth and damage area as a function of the number of shots (λ=1064 nm, 10-ns, 30 J/cm^2) showing the transition between the two damage growth stages.

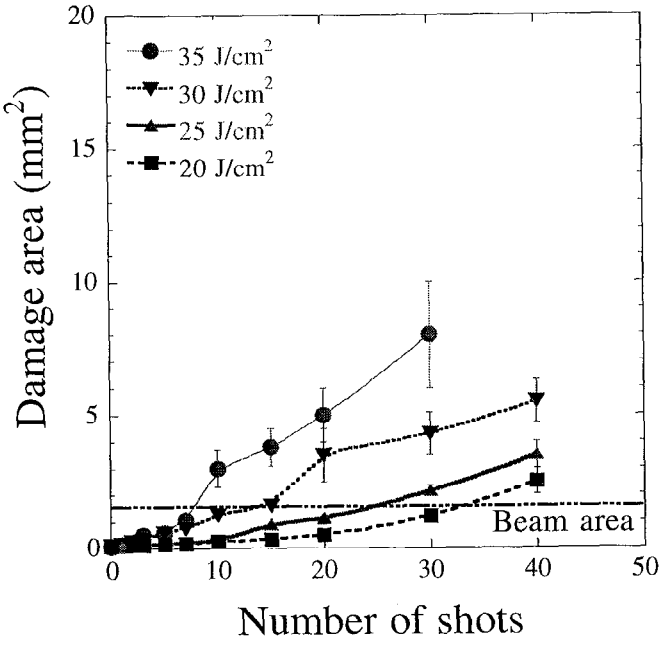

Figure 3: Damage area as a function of the number of shots for various fluences (λ=1064 nm, 10-ns).

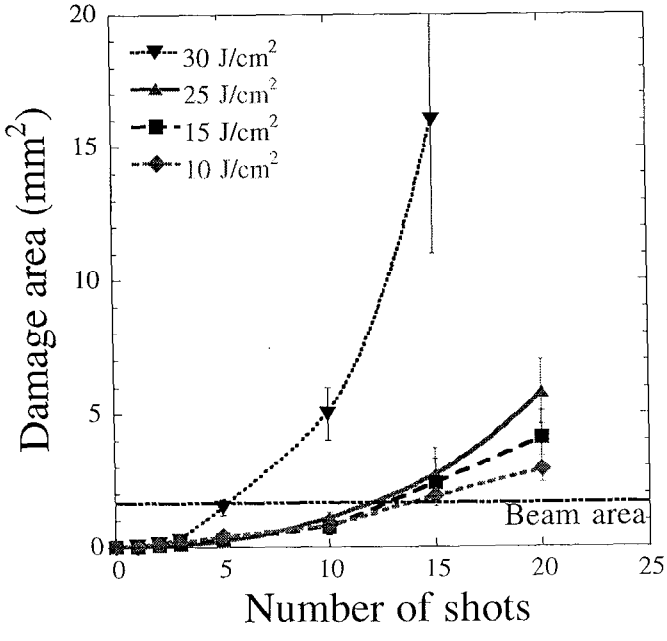

Figure 4: Damage area as a function of the number of shots for various fluences (λ=355 nm, 8-ns).

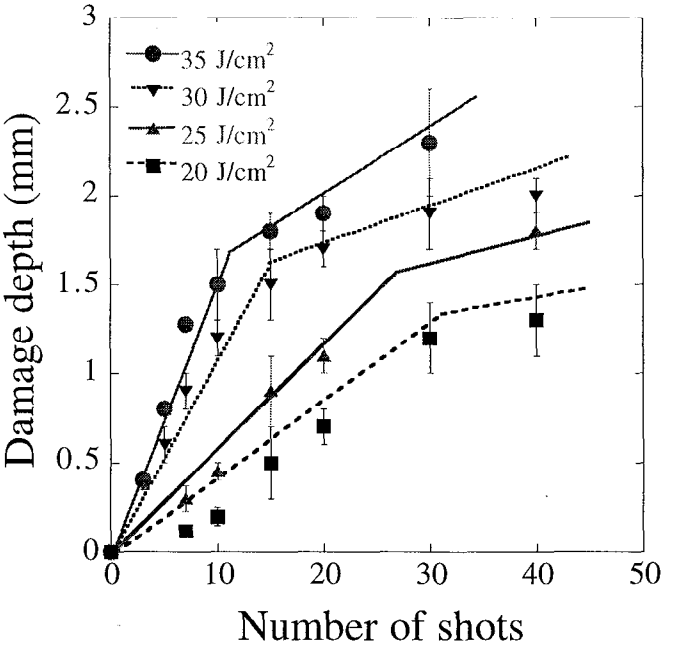

Figure 5: Damage depth as a function of the number of shots for various fluences (λ=1064 nm, 10-ns).

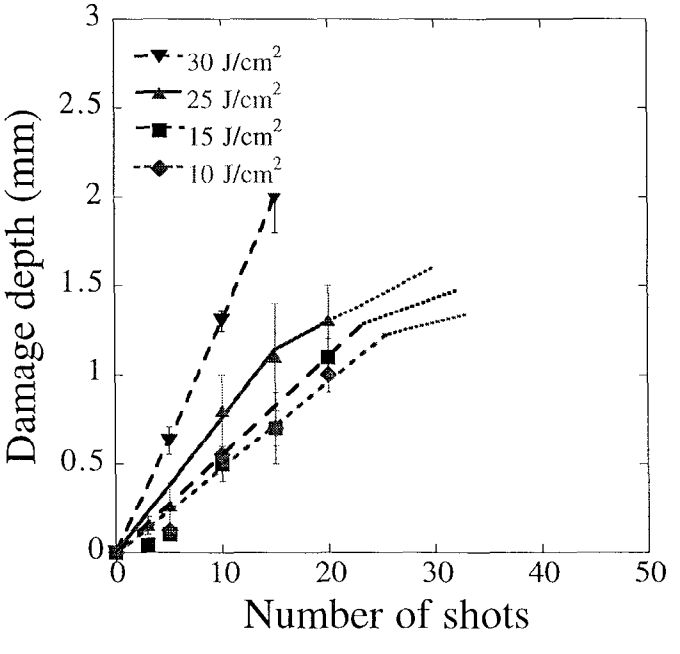

Figure 6: Damage depth as a function of the number of shots for various fluences (λ=355 nm, 8-ns).

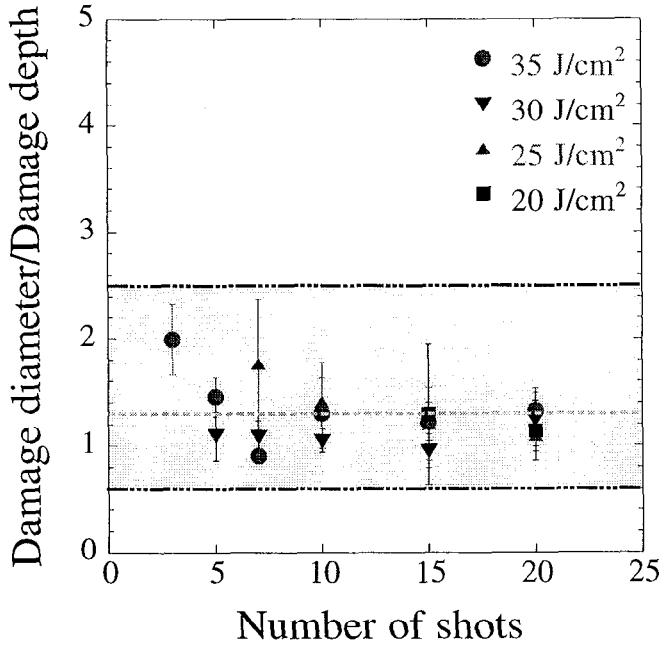

Figure 7: Damage aspect ratio as a function of the number of shots during stage I (λ=1064 nm, 10-ns). At 1064 nm the average aspect ratio is 1.3±0.3.

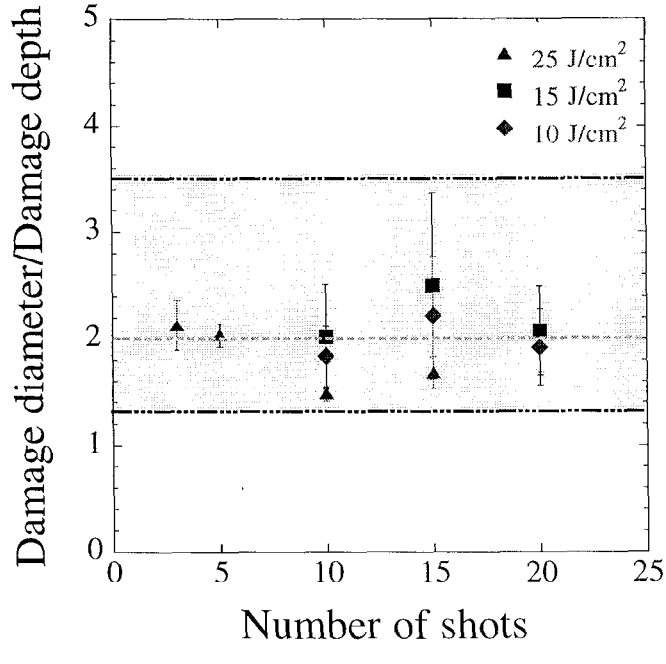

Figure 8: Damage aspect ratio as a function of the number of shots during stage I (λ=355 nm, 8-ns). At 355 nm the average aspect ratio is 2.0±0.3.

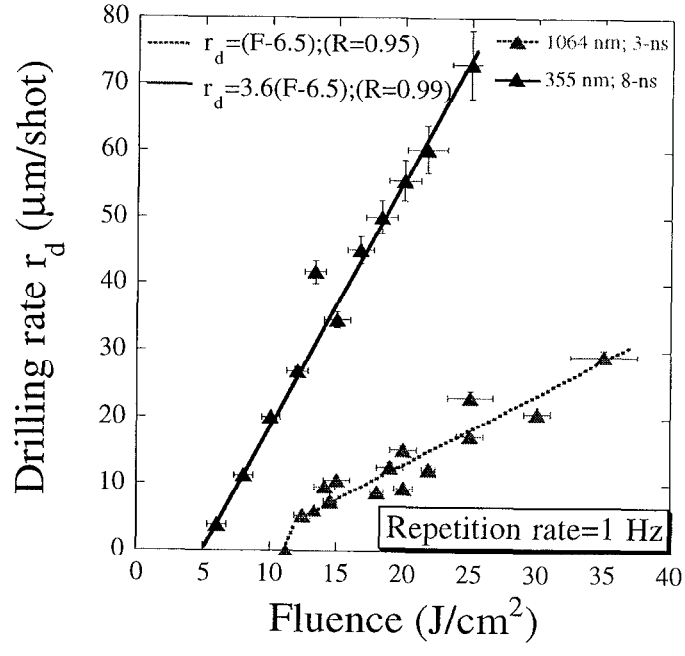

Figure 9: Stage II drilling rate as a function of fluence at 1064 and 355 nm. Damage was initiated at a mechanical flaw.

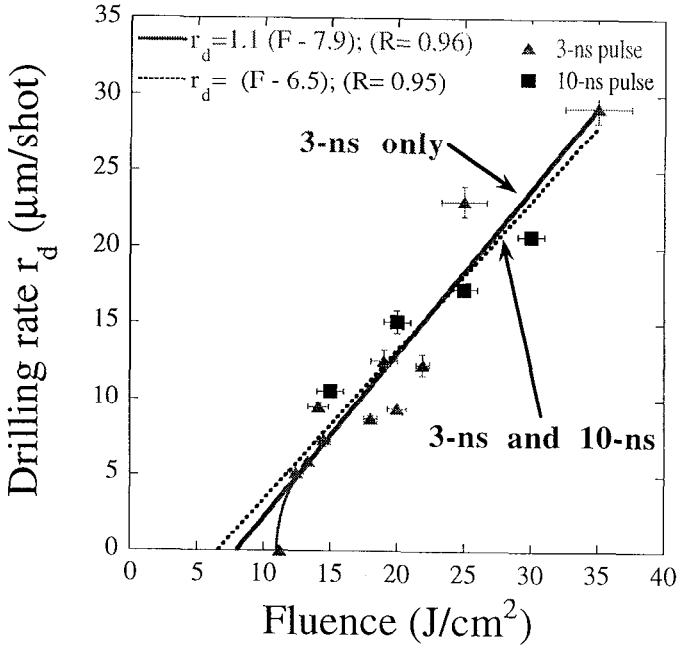

Figure 10: Drilling rate as a function of fluence at different pulse-widths (λ=1064 nm). The data obtained with a 3-ns pulse lie on the same line fit than those obtained with a 10-ns pulse.

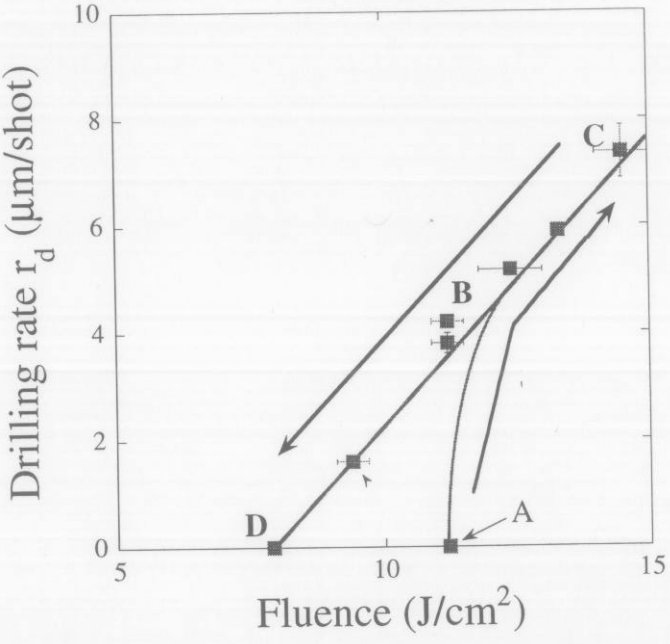

Figure 11: Hysteresis of the drilling rate as a function of fluence at 1064 nm (10-ns pulse). Drilling began to occur at a mechanical flaw at about 11 J/cm^2 (point A).

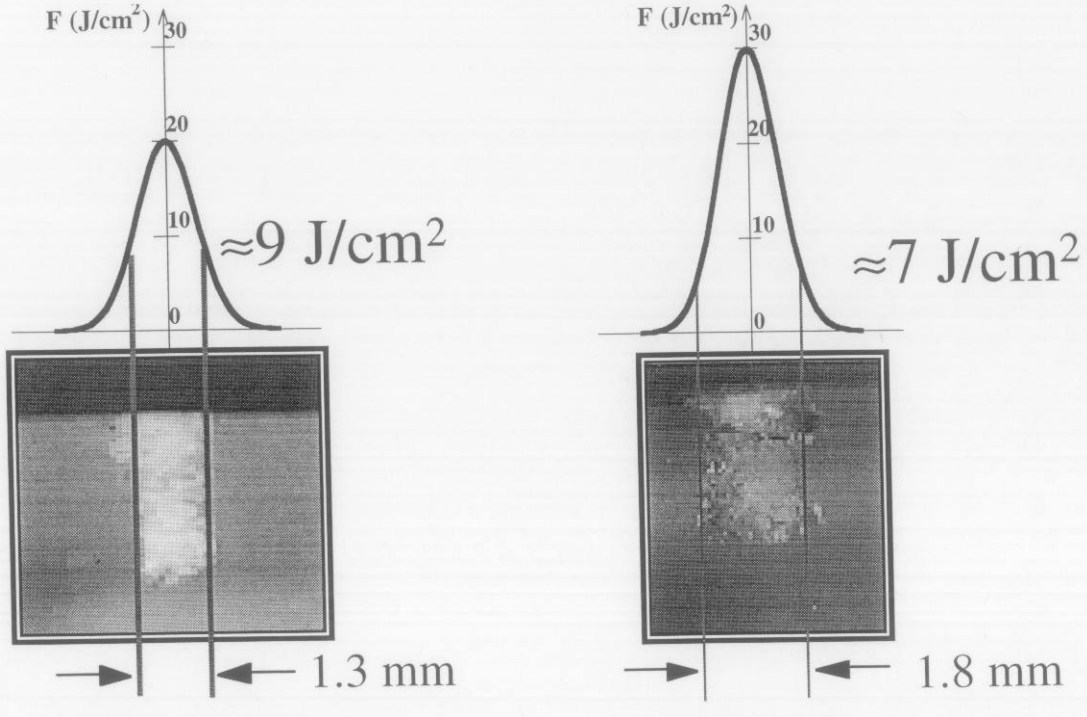

Figure 12: Drilling morphology at 1064 nm: 300 shots at 20 J/cm^2 (left) and 100 shots at 30 J/cm^2 (right). The figure shows that in both cases the rim of the channel was irradiated at about 8 J/cm^2.

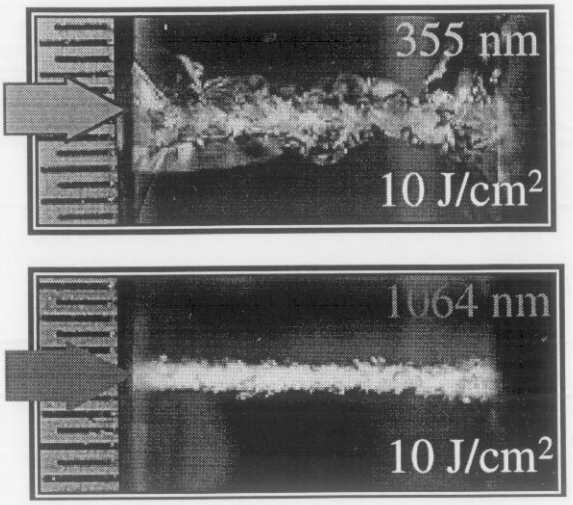

Figure 13: Drilling morphology at 1064 nm (left) and 355 nm (right). The arrow indicates the $1/e^2$ diameter of the beam (1.5 mm at both wavelengths).

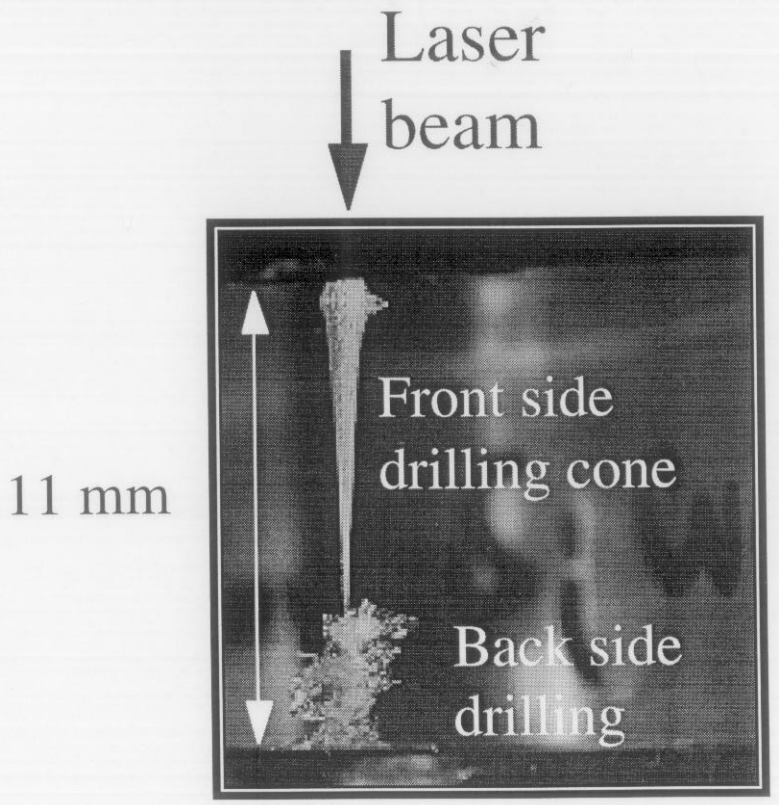

Figure 14: Front side drilling morphology. The drilled cone has been produced at 355 nm by more than 20,000 shots at 45 J/cm^2.

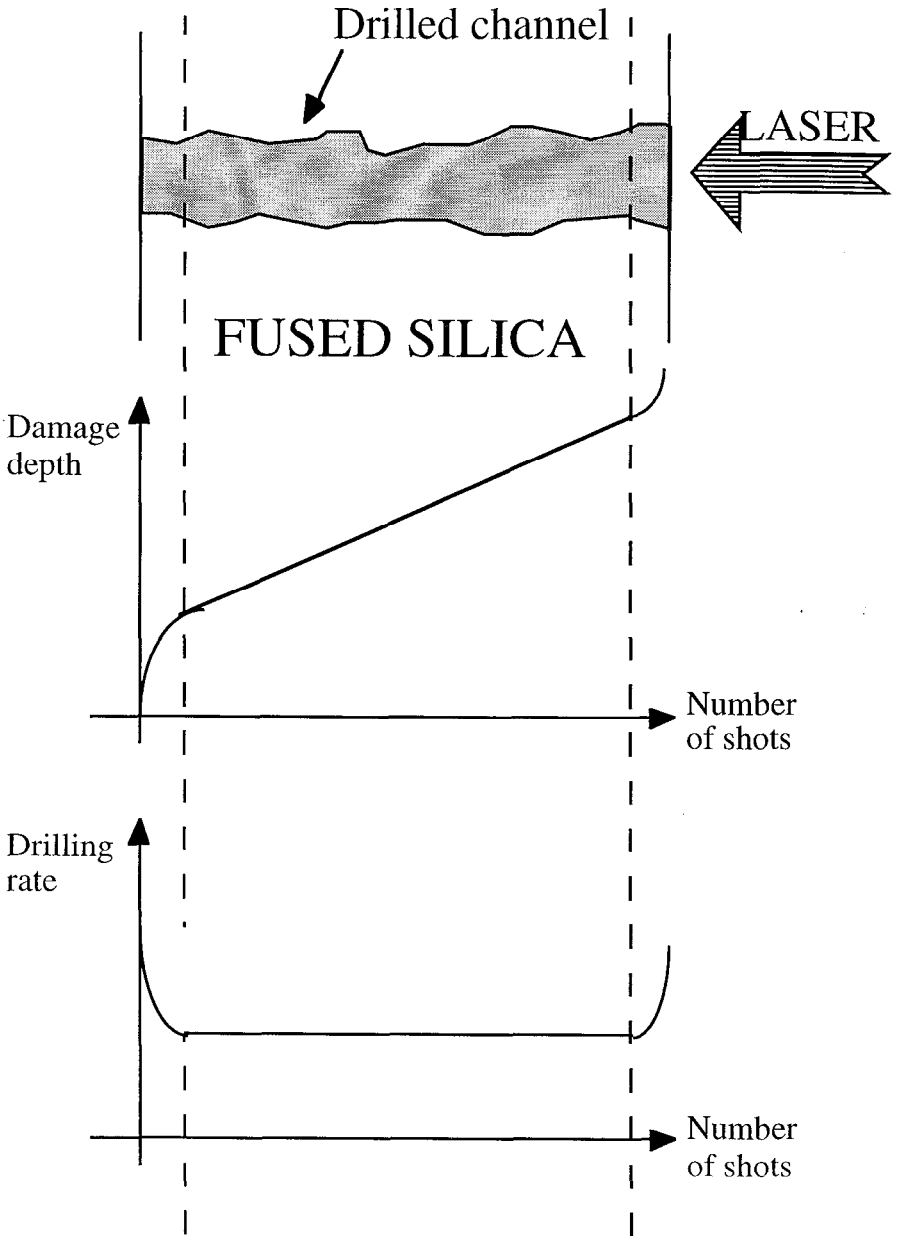

Figure 15: Qualitative behavior of the drilling rate changes during a drilling experiment. The drilling rates are always higher close to the surfaces (at the beginning and at the end of the experiment).

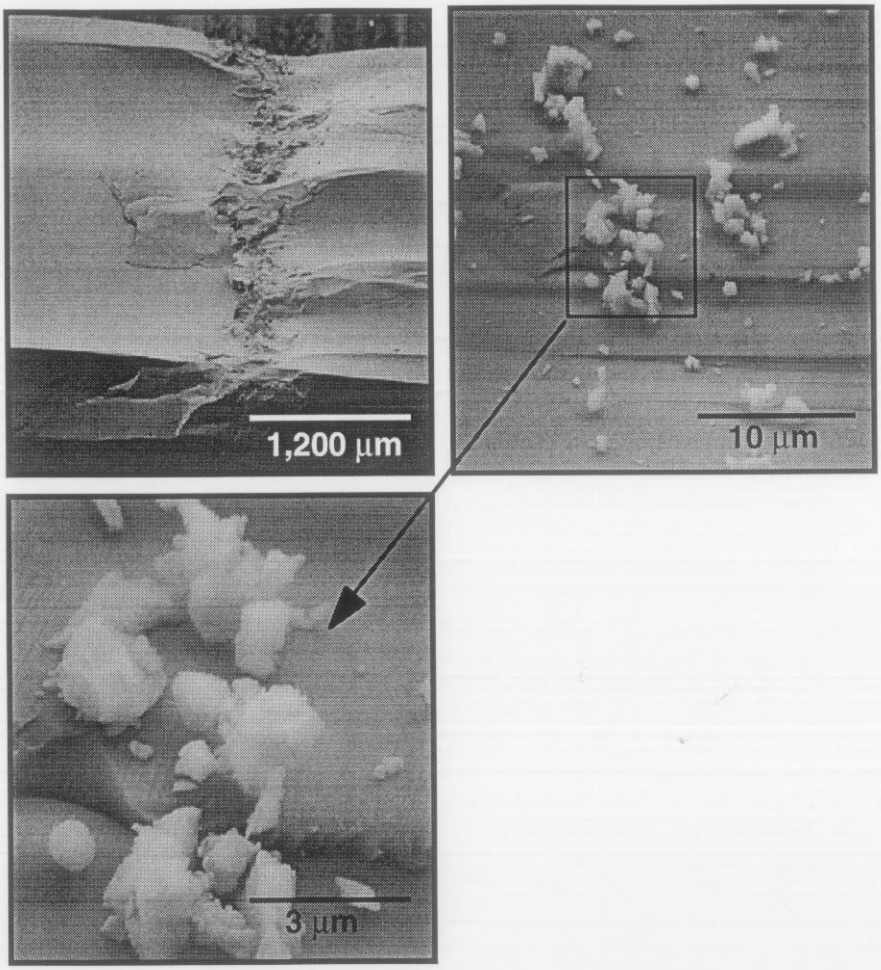

Figure 16: SEM micrographs of the debris found inside a channel drilled at 1064 nm.